

Diana Belotti, Florian Kampert, Mareike C. Jahnke and F. Ekkehardt Hahn*

Oxidative addition of a 8-bromotheobromine derivative to d^{10} metals

<https://doi.org/10.1515/zn-2021-0011>

Received January 26, 2021; accepted February 5, 2021;
published online March 4, 2021

Abstract: Reaction of 8-bromo-7-ethyl-3-methylxanthine **1** with zerovalent group 10 metal complexes gave via an oxidative addition of the C–Br bond the neutral complexes *trans*-[**2**] (M = Pd) and *trans*-[**3**] (M = Pt) bearing a theobromine-derived azolato ligand. While the oxidative addition to [Pd⁰(PPh₃)₄] gave exclusively *trans*-[**2**], the reaction with the more substitution-inert [Pt⁰(PPh₃)₄] yielded after 1 day the kinetic product *cis*-[**3**], which was converted under heating for a total of 3 days completely into the thermodynamically more stable complex *trans*-[**3**]. Treatment of *trans*-[**2**], *trans*-[**3**] or the mixture of *cis*/*trans*-[**3**] with the proton source HBF₄·Et₂O led to complexes *trans*-[**4**]BF₄, *trans*-[**5**]BF₄ and a mixture of *cis*/*trans*-[**5**]BF₄ with retention of the original ratio of *cis* to *trans*, respectively. The molecular structures of the azolato complexes *trans*-[**2**] and *trans*-[**3**] and of the theobromine derived *p*NHC complexes *trans*-[**4**]BF₄ and *trans*-[**5**]BF₄ have been determined by X-ray diffraction studies.

Keywords: N-heterocyclic carbene; oxidative addition; palladium; platinum.

1 Introduction

N-Heterocyclic carbenes (NHCs) featuring two alkyl or aryl substituents at the ring-nitrogen atoms are ubiquitous ligands in organometallic chemistry [1–3]. The enormous variety of NHC ligands, their different steric and electronic properties and the general stability of the M–C_{NHC} bonds allow for multiple applications of NHCs and their complexes, such as catalysts for selected transformations

[4–6], in metallodrugs [7] or as building blocks in supramolecular assemblies [8, 9]. A modification of the NHC ligand after complex formation is not possible for most complexes bearing NR,NR-substituted NHCs. Such post-synthetic modifications of NHC ligands require, for example, an unsubstituted or protonated ring-nitrogen atom of the diazaheterocycle. Protic NHC ligands (*p*NHCs) [10–12] feature one or two protonated ring-nitrogen atoms. Coordinated *p*NHCs can be deprotonated at the ring-nitrogen atoms. Subsequent N-alkylation leads to new NHC ligands [13, 14]. In addition, complexes bearing a *p*NHC ligand are potentially suitable for substrate binding and orientation through N–H...substrate hydrogen bonds [15–18].

Generally, access to complexes bearing *p*NHC ligands is limited [10–12]. Most *p*NHC complexes have either been prepared by a template-controlled cyclization of functionalized isocyanides [13] or by the oxidative addition of azoles to complexes of low-valent late transition metals [10–12]. The oxidative addition protocol can follow two strategies. One method is based on the oxidative addition of the C2–H bond of N-alkylazoles to low-valent transition metal complexes with formation of azolato/hydrido complexes followed by a reductive elimination of a proton from the metal center with protonation of the azolato ligand to the *p*NHC ligand [10–12]. This procedure has been employed for the preparation of *p*NHC complexes of various transition metals such as Rh^I [19, 20], Ru^{II} [21–23], Fe⁰ [24], Ir^I [20] or Ir^{III} [23, 25]. The oxidative addition of neutral azoles is often limited to azoles bearing an N-bound donor, which pre-coordinates to the metal center and thus facilitates the subsequent C2–H oxidative addition [25]. In contrast to the C2–H oxidative addition, the C2–X oxidative addition of 2-halogenoazoles proceeds in the absence of an additional donor function bound to the azole. While first reports of the oxidative addition of azole C2–X bonds by Roper appeared as early as 1973 [26, 27], this procedure has recently received renewed attention [10–12, 28]. Several complexes bearing protic NH,NH- [14, 29] or NH,NR-NHC ligands [28, 30] have been described. Apart from *p*NHC ligands obtained from the ubiquitous 2-halogenoimidazole or 2-halogenobenzimidazole NHC precursors [28, 30], protic MIC (MIC = mesoionic carbene) [31, 32] and CAAC ligands [33] are also known. Finally, biomolecules such as

*Corresponding author: F. Ekkehardt Hahn, Institut für Anorganische und Analytische Chemie der Westfälischen Wilhelms-Universität Münster, Corrensstraße 30, D-48149 Münster, Germany, E-mail: fehahn@uni-muenster.de

Diana Belotti, Florian Kampert and Mareike C. Jahnke, Institut für Anorganische und Analytische Chemie der Westfälischen Wilhelms-Universität Münster, Corrensstraße 30, D-48149 Münster, Germany

8-halogenocaffeine [29, 34, 35] or -adenine [35, 36] have been employed in oxidative addition reactions to yield complexes with *p*NHC ligands.

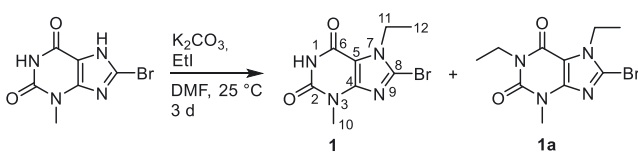
The oxidative addition of 8-halogenocaffeine and -adenine to $[\text{Pt}(\text{PPh}_3)_4]$ yielded exclusively the complexes with a *trans* arrangement of the PPh_3 ligands [35], while the oxidative addition of 2-chlorobenzimidazole to Pt^0 yielded a mixture of *cis*- and *trans*- PPh_3 complexes [28]. We became interested in the factors governing the product distribution in the oxidative addition of halogenoazoles to Pd^0 and Pt^0 . Next to the reaction temperature and duration, the type of halogenoazole appears to be a factor. The purine base theobromine is structurally related to caffeine but the electronic situation is slightly different due to a variation in the N-substitution of the pyrimidine ring. In this contribution we present the results obtained from the oxidative addition of a 8-bromotheobromine derivative to Pd^0 and Pt^0 complexes.

2 Results and discussion

2.1 Synthesis and characterization of 8-bromo-7-ethyl-3-methylxanthine 1

The NHC precursor 8-bromo-7-ethyl-3-methylxanthine **1** was synthesized by alkylation of 8-bromo-3-methylxanthine [37] with 1.1 equivalents of ethyl iodide in the presence of K_2CO_3 as base (Scheme 1). Next to **1**, the formation of the doubly N1,N7 di-alkylated byproduct **1a** (ratio **1**:**1a** = 1:0.4) was observed. Compound **1** was separated by column chromatography and isolated in 40% yield.

Formation of the ligand precursor **1** was confirmed by NMR spectroscopy, mass spectrometry and by elemental analyses. In the ^1H NMR spectrum of **1** the resonances for the CH_2 and CH_3 groups of the N7 bound ethyl substituent are detected as quartet and triplet at $\delta = 4.34$ and 1.41 ppm, respectively. The characteristic resonances in the $^{13}\text{C}\{^1\text{H}\}$ NMR spectrum of **1** are observed at $\delta = 153.9$ (C6), 151.1 (C2) and 127.5 ppm (C8). The resonances of the carbon atoms of the N7 bound ethyl substituent were detected at $\delta = 43.3$ (CH_2 , C11) and 15.7 ppm (CH_3 , C12).



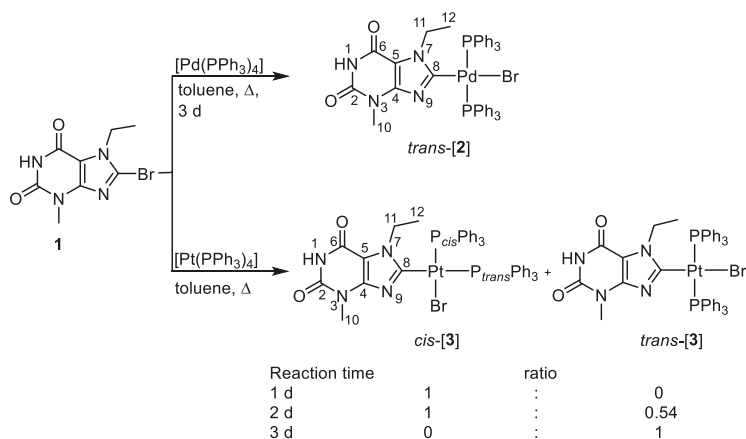
Scheme 1: Synthesis of 8-bromo-7-ethyl-3-methylxanthine **1**.

2.2 Synthesis and characterization of complexes *trans*-[**2**] and *trans*-[**3**]

Treatment of $[\text{Pd}(\text{PPh}_3)_4]$ with an equimolar amount of **1** in boiling toluene for 3 days yielded complex *trans*-[**2**] as a colorless solid in 67% yield. Under identical conditions, ligand precursor **1** reacted with $[\text{Pt}(\text{PPh}_3)_4]$ to give the colorless complex *trans*-[**3**] in 54% yield (Scheme 2). However, when the reaction time was decreased to one day, complex *cis*-[**3**] was isolated instead. Complex *cis*-[**3**] is the kinetic product of the oxidative addition reaction of **1** to $[\text{Pt}(\text{PPh}_3)_4]$. After two days reaction time a mixture of *cis*-[**3**] and the thermodynamically more stable *trans*-[**3**] in a ratio of 1 to 0.54 was observed. After a reaction time of three days, the only observed product was complex *trans*-[**3**].

Both the Pd^{II} and the Pt^{II} complexes bear a C8-bound negatively charged theobromine-derived azolato ligand with an unsubstituted nitrogen atom. The formation of dinuclear species was not observed, contrary to the results reported for the oxidative addition of 2-halogenated benzimidazole derivatives to zero-valent group 10 metals in the absence of a proton source [28]. The mode of reactivity found for 8-bromotheobromine is in good agreement with the observations made for similar purine bases such as caffeine or other theophylline derivatives [29, 34, 35, 38], where the 8-halogenated derivatives oxidatively add to $[\text{Pd}(\text{PPh}_3)_4]$ or $[\text{Pt}(\text{PPh}_3)_4]$ leading exclusively to the mononuclear complexes. This observation can be rationalized with the reduced electron density within the five-membered heterocycle due to the electron-withdrawing nature of the annelated ring system together with the steric demand of the azolato ligand [38]. The formation of a *cis*-configured platinum(II) complex was not observed previously in the oxidative reaction of halogenated purine bases.

The azolato complexes were characterized by NMR spectroscopy. Interestingly, the resonance for proton H1 (bond to atom N1) in the ^1H NMR spectrum was detected at $\delta = 8.44$ (*trans*-[**2**]) and 8.28 ppm (*trans*-[**3**]). These resonances are shifted up-field compared to the H1 resonance in free **1** ($\delta = 8.72$ ppm), which we attribute to the negative charge of the azolato ligands in the complexes. The other ^1H NMR resonances for *trans*-[**2**] and *trans*-[**3**] fall in the expected range. The $^{13}\text{C}\{^1\text{H}\}$ NMR spectra exhibit resonances at $\delta = 163.7$ (*t*, $^2J_{\text{CP}} = 3.5$ Hz) and 151.7 (*t*, $^2J_{\text{CP}} = 9.8$ Hz) ppm for the C8 carbon atoms in *trans*-[**2**] and (*trans*-[**3**]), respectively. As expected, the chemical shift of C8 is shifted significantly upon metal coordination ($\delta(\text{C8}) = 127.5$ ppm in **1**). The chemical shifts for C8 in *trans*-[**2**] and *trans*-[**3**] compare well to the chemical shifts reported for the C8



Scheme 2: Synthesis of Pd^{II} complex *trans*-[2] and Pt^{II} complexes *cis*-/*trans*-[3].

carbon atom in related Pd^{II} and Pt^{II} complexes bearing a C8-bound xanthine-derived azolato ligand [29, 34, 35]. The triplet resonances observed for C8 in *trans*-[2] or *trans*-[3] indicate the *trans* arrangement of the phosphine donors in these complexes. The *trans* configuration can also be concluded from the observation of only one resonance in the ³¹P{¹H} NMR spectra at $\delta = 21.5$ ppm (s) for *trans*-[2] and $\delta = 18.7$ ppm (s, Pt satellites, $^1J_{\text{PPt}} = 2769$ Hz) for *trans*-[3].

A comparison of the NMR data of the Pt^{II} isomers *cis*-[3] and *trans*-[3] reveals significant differences. The resonance of the C8 carbon atom in *cis*-[3] was detected as a doublet of doublets at $\delta = 167.6$ ppm (*dd*, $^2J_{\text{CP}(\text{trans})} = 148.9$ Hz, $^2J_{\text{CP}(\text{cis})} = 9.5$ Hz) caused by the two chemically different phosphorus atoms. A significant difference between $^2J_{\text{CP}(\text{trans})}$ and $^2J_{\text{CP}(\text{cis})}$ has previously been reported for related complexes of the type [M(azolato)(PPh₃)₂(X)] [28]. In addition, the C8 resonance in *cis*-[3] is shifted significantly downfield compared to the C8 resonance in *trans*-[3] ($\delta = 151.7$ ppm).

The ³¹P{¹H} NMR spectrum of *cis*-[3] reveals two resonances at $\delta = 15.3$ ppm (*d*, $^2J_{\text{PP}} = 17.9$ Hz, Pt satellites $^1J_{\text{PPt}} = 1973$ Hz, P_{*trans*}Ph₃) and at $\delta = 12.6$ ppm (*d*, $^2J_{\text{PPt}} = 18.0$ Hz, Pt satellites $^1J_{\text{PPt}} = 3970$ Hz, P_{*cis*}Ph₃). Due to the *cis* arrangement of the PPh₃ ligands in *cis*-[3], rotation about the Pt–C8 bond is restricted and diastereotopic behavior was observed for the two methylene protons of the N7-bound ethyl substituent leading to two separated resonances for these protons at $\delta = 4.66$ ppm (*dq*, $^2J_{\text{HH}} = 14$ Hz, $^3J_{\text{HH}} = 7.1$ Hz, 1H, H11a) and $\delta = 4.13$ ppm (*dq*, $^2J_{\text{HH}} = 14$ Hz, $^3J_{\text{HH}} = 7.1$ Hz, 1H, H11b).

In addition to NMR spectroscopy, the formation of *trans*-[2] and *trans*-[3] was also indicated by HR mass spectrometry (ESI, positive ions). The mass spectra exhibited the peaks of highest intensity for *trans*-[2] at $m/z = 905.0845$ (calcd. for [*trans*-[2]+H]⁺ 905.0848) and for *trans*-[3] at $m/z = 993.1456$ (calcd. 993.1451 for [*trans*-[3]+H]⁺).

Crystals of *trans*-[2]·2CH₂Cl₂ and *trans*-[3]·2CH₂Cl₂ were obtained by slow diffusion of diethyl ether into a saturated dichloromethane solution of the respective complex. The molecular structures of complexes *trans*-[2] and *trans*-[3] are depicted in Figure 1.

In both complexes the azolato ligand is oriented essentially perpendicular to the PdBrP₂ plane, while the two PPh₃ ligands are arranged in the expected *trans* orientation. The M–C8 bonds lengths (Pd–C8 1.980(2) Å, Pt–C8 1.982(3) Å) are identical within experimental error. However, the M–Br bond lengths are slightly different with the longer one observed for the Pt–Br bond. This order is reversed for the M–P bond lengths, where the shorter distances are observed for the Pt–P bonds. However, all bond lengths and angles involving the metal atoms fall in the range previously described for Pd^{II} and Pt^{II} complexes bearing xanthine-derived azolato ligands [34, 35, 38].

Notably, and in accord with previous observations [34, 35, 38], the N9–C8 bonds in both complexes (*trans*-[2] 1.347(3) Å, *trans*-[3] 1.351(4) Å) are shorter than the N7–C8 bond lengths (1.365(3) and 1.366(4) Å), although the differences in the N–C8 distances ($\Delta\delta < 0.02$ Å) are smaller than the difference in the N–C_{azolato} bond lengths observed for a Pt-benzimidazolato complex ($\Delta\delta \approx 0.07$ Å) [39]. The difference in the N–C bond lengths can be attributed to the negative charge at atom N9 which, however, is smaller in the xanthine derived azolato ligands compared to the benzimidazolato ligand due to the electron withdrawing nature of the annelated heterocycles.

While the formation of dinuclear complexes via attack of the unsubstituted azolato ring-nitrogen atom at the metal atom of a second complex molecule was not observed for *trans*-[2] and *trans*-[3], these complexes still form dinuclear aggregates via the formation of N1–H···O2 hydrogen bonds (Figure 2). Related hydrogen bonds have been observed in azolate complexes obtained by oxidative addition of 8-halogenoguanosine derivatives to [Pd(PPh₃)₄] [36].

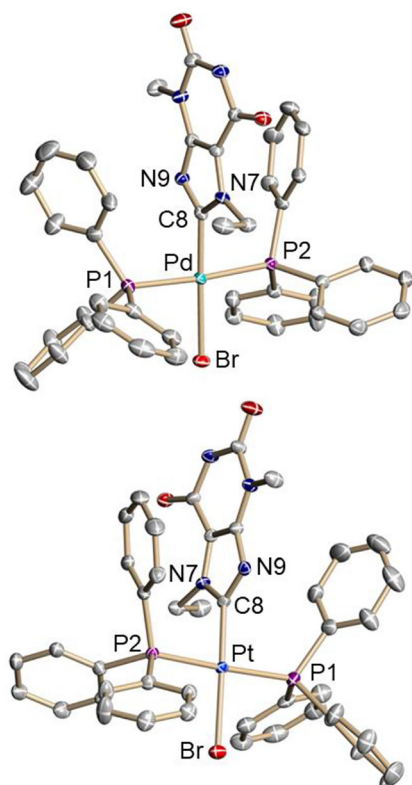


Figure 1: Molecular structures of *trans*-[2] in crystals of *trans*-[2]·2CH₂Cl₂ (top) and *trans*-[3] in crystalline *trans*-[3]·2CH₂Cl₂ (bottom). Hydrogen atoms have been omitted for clarity and 50% displacement ellipsoids are depicted. Selected bond lengths (Å) and angles (deg) for *trans*-[2] [*trans*-[3]]: M–Br 2.4882(3) [2.4943(4)], M–P1 2.3334(6) [2.3169(9)], M–P2 2.3416(6) [2.3241(9)], M–C8 1.980(2) [1.982(3)], N7–C8 1.365(3) [1.366(4)], N9–C8 1.347(3) [1.351(4)]; Br–M–P1 91.080(2) [90.10(3)], Br–M–P2 92.72(2) [91.71(2)], Br–M–C8 176.65(7) [177.38(10)], P1–M–P2 175.19(2) [176.73(3)], P1–M–C8 88.70(6) [89.77(10)], P2–M–C8 87.68(6) [88.54(10)], N7–C8–N9 111.5(2) [111.1(3)].

2.3 Synthesis and characterization of complexes *trans*-[4]BF₄ and *trans*-[5]BF₄

Treatment of complexes *trans*-[2] and *trans*-[3] with HBF₄·Et₂O yielded complexes *trans*-[4]BF₄ and *trans*-[5]BF₄ in reasonable yields via protonation of the N9 ring-nitrogen atom (Scheme 3). Thus complexes *trans*-[4]BF₄ and *trans*-[5]BF₄ bear a theobromine-derived *p*NHC ligand. Interestingly, these complexes cannot be prepared in a one-pot reaction by treating the C8-halogenated xanthine derivative with [M(PPh₃)₄] in the presence of a mild acid such as NH₄BF₄ [28, 29]. This difference in reactivity can be attributed to the electron withdrawing theobromine system, which leads for complexes *trans*-[2] and *trans*-[3] to a decreased basicity of the unsubstituted ring-nitrogen atom of the azolato ligand.

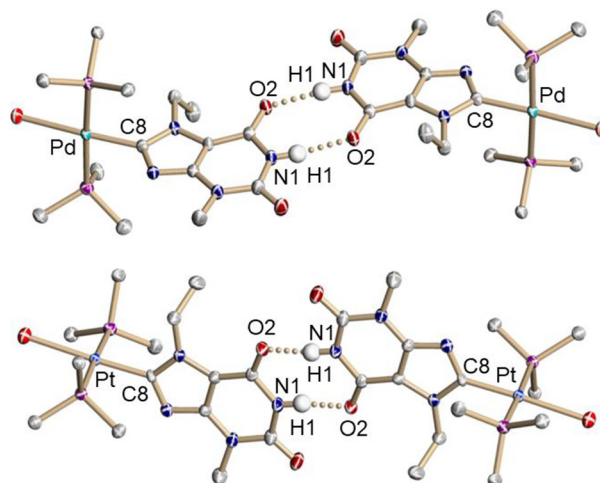
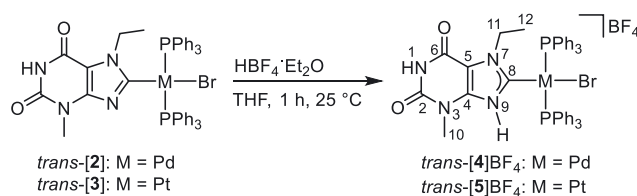


Figure 2: Hydrogen bonds between two molecules of *trans*-[2] (top) and *trans*-[3] (bottom) in the crystal structures of *trans*-[2]·2CH₂Cl₂ and *trans*-[3]·2CH₂Cl₂, respectively. Displacement ellipsoids are drawn at the 50% probability level. Hydrogen atoms except for H1 have been omitted for clarity. Selected bond lengths (Å) and angles (deg) for *trans*-[2] [*trans*-[3]]: O2...N1 2.828 [2.821], O2...H–N1 169.7 [168.2].

The NMR spectra of *trans*-[4]BF₄ and *trans*-[5]BF₄ are similar to those of the parent azolato complexes *trans*-[2] and *trans*-[3], respectively. The only exceptions are the resonances at $\delta = 11.25$ (*trans*-[4]BF₄) and $\delta = 10.41$ ppm (*trans*-[5]BF₄) in the ¹H NMR spectra for the NH protons of the *p*NHC ligands. The ¹³C{¹H} NMR spectra exhibit the resonances of the carbene carbon atom C8 as triplet at $\delta = 164.9$ ppm (²J_{CP} = 9.4 Hz) and at $\delta = 151.7$ ppm (²J_{CP} = 10.1 Hz) for *trans*-[4]BF₄ and *trans*-[5]BF₄, respectively. These chemical shifts are close to those observed for the C8 carbon atoms of the parent complexes *trans*-[2] ($\delta = 163.7$ ppm) and *trans*-[3] ($\delta = 151.7$ ppm). The ³¹P{¹H} NMR spectra of both complexes exhibit the resonances of the two chemically equivalent phosphorus atoms as singlets at $\delta = 21.0$ ppm (*trans*-[4]BF₄) and $\delta = 16.6$ ppm (*trans*-[5]BF₄). In addition, for *trans*-[5]BF₄, Pt satellites were observed (¹J_{Pt} = 2464 Hz). Interestingly, the ¹J_{Pt} coupling constant in cationic *trans*-[5]⁺ is smaller than



Scheme 3: Synthesis of the Pd^{II} and Pt^{II} complexes *trans*-[4]BF₄ and *trans*-[5]BF₄.

that in neutral *trans*-[3] ($^1J_{\text{Pt}} = 2769$ Hz). A similar trend in the coupling constant upon the transition from the azolato to the *p*NHC complexes has been observed for *trans*-Pt^{II} complexes bearing caffeine-derived NHC ligands [35]. A triplet was observed in the $^{195}\text{Pt}\{^1\text{H}\}$ NMR spectrum of *trans*-[5]BF₄ at $\delta = -4500.4$ ppm ($^1J_{\text{Pt}} = 2464$ Hz). HR mass spectrometry (ESI, positive ions) showed the strongest peaks for the cation *trans*-[4]⁺ at $m/z = 905.0842$ (calcd. 905.0848 for [*trans*-[4]]⁺) and for *trans*-[5]⁺ at $m/z = 993.1445$ (calcd. 993.1451 for [*trans*-[5]]⁺).

The composition and geometry of *trans*-[4]BF₄ and *trans*-[5]BF₄ were verified by X-ray diffraction studies with crystals of composition *trans*-[4]BF₄ and *trans*-[5]BF₄·

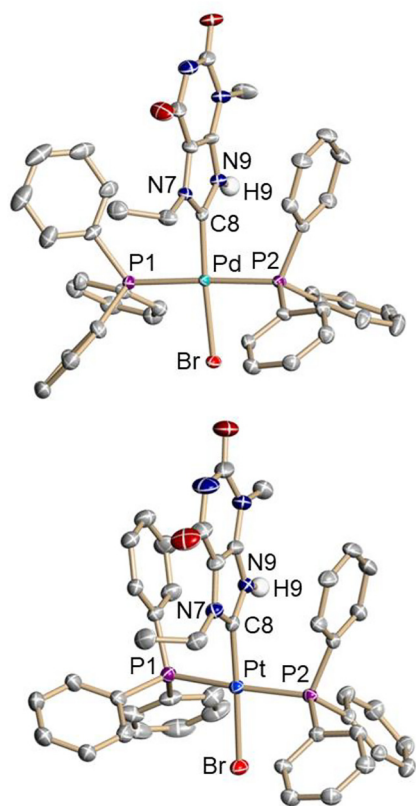


Figure 3: Molecular structures of one of the two independent complex cations *trans*-[4]⁺ (top) in *trans*-[4]BF₄ and of *trans*-[5]⁺ (bottom) in *trans*-[5]BF₄·Et₂O. Hydrogen atoms except for H9 have been omitted for clarity and displacement ellipsoids are drawn at the 50% probability level. Selected bond lengths (Å) and angles (deg) of cation *trans*-[4]⁺ [*trans*-[5]⁺]: M–Br 2.4602(4) [2.4685(4)], M–P1 2.3627(9) [2.3233(9)], M–P2 2.3212(9) [2.3155(9)], M–C8 1.988(3) [1.982(3)], N7–C8 1.338(4) [1.340(5)], N9–C8 1.361(4) [1.352(4)]; Br–M–P1 89.56(2) [90.22(2)], Br–M–P2 88.08(2) [89.61(2)], Br–M–C8 176.48(10) [177.28(10)], P1–M–P2 177.46(3) [171.66(3)], P1–M–C8 93.91(10) [89.42(10)], P2–M–C8 88.46(10) [91.14(10)], N7–C8–N9 106.9(3) [107.2(3)].

Et₂O, respectively. The asymmetric unit of *trans*-[4]BF₄ contains two essentially identical formula units. Only one of the complex cations in the asymmetric unit of *trans*-[4]⁺ is depicted in Figure 3 (top) together with the complex cation of *trans*-[5]⁺ (bottom).

The major differences in the metric parameters of the *p*NHC complex cations *trans*-[4]⁺ and *trans*-[5]⁺ relative to the parent azolato complexes *trans*-[2] and *trans*-[3] were observed in the five-membered diazaheterocycles. While the M–C8 bond lengths in the *p*NHC complexes are identical within experimental error (*trans*-[4]BF₄ 1.988(3) Å, *trans*-[5]BF₄ 1.982(3) Å), they are also unchanged from the bond lengths in the neutral azolato complexes (*trans*-[2] 1.980(2) Å and *trans*-[3] 1.982(3) Å). A significant change was observed for the N–C8 bonds upon N9 protonation. While the azolato complexes *trans*-[2] and *trans*-[3] (Figure 1) feature shorter N9–C8 and longer N7–C8 bonds, the protonation to *trans*-[4]BF₄ and *trans*-[5]BF₄ leads to almost identical N–C8 separations. Even more significant is the reduction of the N7–C8–N9 angle upon N9 protonation (*trans*-[4]BF₄ 106.9(3)°, *trans*-[5]BF₄ 107.2(3)°) compared to the azolato complexes (*trans*-[2] 111.5(2)°, *trans*-[3] 111.1(3)°) which is in accord with previous observations [34, 35].

The crystal structure of *trans*-[4]BF₄ reveals two hydrogen bond interactions of the complex cation with two BF₄[−] anions via the N9–H and N1–H groups (distances N9...F3 2.725 Å, N1...F2 2.842 Å), leading to chains of cations in the solid state (Figure 4). For *trans*-[5]BF₄·Et₂O the N1–H proton interacts with the co-crystallized diethyl ether molecule (distance N1...O 3.054 Å).

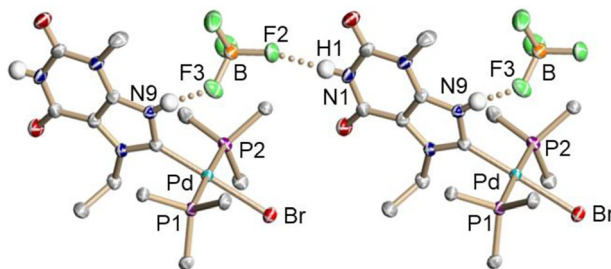


Figure 4: Intermolecular interactions in the crystal structure of *trans*-[4]BF₄. Displacement ellipsoids are drawn at the 50% probability level. Hydrogen atoms, except for N1–H and N9–H, have been omitted for clarity. Selected hydrogen bond lengths (Å): N9...F3 2.725 Å, N1...F2 2.878 Å.

2.4 Synthesis and characterization of a mixture of platinum complexes *cis*/*trans*-[5]BF₄

The mixture of complexes *cis*-/*trans*-[3] (1: 0.54, obtained after 2 days reaction time, Scheme 2) was suspended in THF and HBF₄·Et₂O was added dropwise (Scheme 4). This led to the formation of a mixture of complexes *cis*-/*trans*-[5]BF₄, which was isolated in a total yield of 50%. The coexistence of both complexes as well as a constant ratio of complexes (*cis*-[5]BF₄:*trans*-[5]BF₄ = 1:0.54) was confirmed by NMR spectroscopy.

As was observed for the azolato complex *cis*-[3], the NMR data of the *p*NHC complex *cis*-[5]BF₄ differ from those of the *trans*-isomer. Generally, the resonances assigned to *cis*-[5]BF₄ in the ¹H NMR spectrum of the mixture are observed more downfield shifted than those belonging to the *trans*-complex. In addition, the rotation about the Pt–C8 bond in *cis*-[5]BF₄ is hindered leading to diastereotopic methylene protons detected as two doublets of quartets at δ = 4.58 ppm (²J_{HH} = 14 Hz, ³J_{HH} = 7.1 Hz) and at δ = 4.21 ppm (²J_{HH} = 14 Hz, ³J_{HH} = 7.1 Hz). In the ¹³C{¹H} NMR spectrum of the complex mixture, the resonances of the carbene carbon atoms are well separated. While the resonance for the carbon atom C8 of *trans*-[5]BF₄ was detected as a triplet at δ = 151.7 ppm (²J_{CP} = 10.1 Hz), the C8 resonance of the *cis*-isomer was observed more downfield as a doublet of doublets at δ = 164.6 ppm (²J_{CP(trans)} = 145.4 Hz, ²J_{CP(cis)} = 9.6 Hz). The resonance of C8 in *cis*-[5]BF₄ is slightly upfield shifted compared to the C8 resonance in the azolato complex *cis*-[3] (δ = 167.6 ppm). The resonances of the two chemically non-equivalent phosphorus atoms were detected as doublets at δ = 13.1 ppm (P_{trans}) and 11.0 ppm (P_{cis}) both featuring an identical ²J_{PP} = 18.9 Hz coupling constant and the characteristic platinum satellites (¹J_{PPt} = 2286 Hz, P_{trans} and 3652 Hz P_{cis}) in the ³¹P{¹H} NMR spectrum of *cis*-[5]BF₄. These resonances are slightly upfield from the corresponding resonances in *cis*-[3]. The ¹⁹⁵Pt NMR spectrum of the mixture of isomers exhibits a triplet at δ = –4500.4 ppm (¹J_{PPt} = 2464 Hz) for *trans*-[5]BF₄ and a doublet of doublets at δ = –4602.9 ppm (¹J_{Pt(cis)} = 3652, ¹J_{Pt(trans)} = 2286 Hz) for *cis*-[5]BF₄.

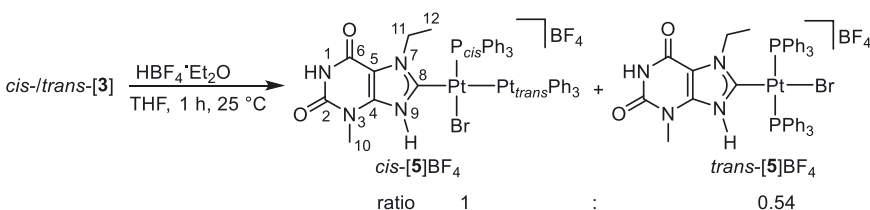
3 Conclusion

We have prepared novel Pd^{II} and Pt^{II} complexes *trans*-[2] and *trans*-[3] bearing a theobromine-derived azolato ligand obtained by the oxidative addition of 8-bromo-N7-ethyl-3-methyl-xanthine **1** to [M⁰(PPh₃)₄] (M = Pd, Pt) followed by protonation at their N9 positions to give the *p*NHC complexes *trans*-[4]BF₄ and *trans*-[5]BF₄. The azolato complexes *trans*-[2] and *trans*-[3] were obtained as the only reaction products after a reaction time of 3 days in boiling toluene. For the reaction of [Pt(PPh₃)₄] with **1**, the effect of a reduction of the reaction time was studied revealing that after only 1 day the isomer *cis*-[3] was the exclusive reaction product, while after 2 days reaction time a mixture of the *cis*/*trans* isomers was obtained in a ratio of 1:0.54. N9-Protonation of *trans*-[2], *trans*-[3] or the mixture of *cis*-/*trans*-[3] (1:0.54) with HBF₄·Et₂O yielded in all cases the complexes bearing the protic theobromine-derived NHC ligand. X-ray diffraction structure determinations revealed for complexes *trans*-[2] and *trans*-[3] an intermolecular interaction between two molecules via N1–H...O2 hydrogen bonds. The *p*NHC complexes *trans*-[4]BF₄ and *trans*-[5]BF₄·Et₂O featured N9–H...F–BF₂–F...H–N1 (*trans*-[4]BF₄) or N1–H...OEt₂ (*trans*-[5]BF₄·Et₂O) hydrogen bonds involving the BF₄[–] anions or the co-crystallized diethyl ether.

4 Experimental section

4.1 General remarks

All manipulations were carried out in an argon atmosphere using standard Schlenk or glovebox techniques. Solvents were dried by standard methods under argon and were freshly distilled prior to use. ¹H, ¹³C{¹H} and ³¹P{¹H} NMR spectra were measured on a Bruker AVANCE I 400 or a Bruker AVANCE III 400 spectrometer. Chemical shifts (δ) are expressed in ppm using the residual protonated solvent signal as internal standard. Coupling constants are expressed in Hertz. Mass spectra were obtained with a Bruker Reflex IV MALDI TOF or an Orbitrap LTQ XL (Thermo Scientific) spectrometer. Elemental analyses were obtained on a Vario EL III CHNS analyzer. The 8-bromo-3-methylxanthine and the metal precursors [M⁰(PPh₃)₄] (M = Pd, Pt) were purchased from commercial sources and were used as received.



Scheme 4: Synthesis of *cis*-/*trans*-[5]BF₄.

4.2 8-Bromo-7-ethyl-3-methylxanthine (1)

8-Bromo-3-methylxanthine (1.200 g, 4.90 mmol) and an excess of potassium carbonate (843 mg, 6.10 mmol) were suspended in DMF (15 mL). Ethyl iodide (0.44 mL, 5.48 mmol) was added to this suspension and the reaction mixture was stirred for 3 days at ambient temperature. The yellowish suspension was poured into ice-cold water (100 mL) and stirred for 1 h at 0 °C. The formed precipitate was isolated by filtration, washed with water and dried *in vacuo*. The residue was purified by column chromatography (SiO₂, CH₂Cl₂:MeOH 100:5) to give **1** after drying *in vacuo* as a colorless solid. Yield: 535 mg (1.96 mmol, 40%). – ¹H NMR (400 MHz, CD₂Cl₂, ppm): δ = 8.72 (s, 1 H, H1), 4.34 (q, ³J_{HH} = 7.1 Hz, 2 H, H11), 3.47 (s, 3 H, H10), 1.41 (t, ³J_{HH} = 7.1 Hz, 3 H, H12). – ¹³C{¹H} NMR (101 MHz, CD₂Cl₂, ppm): δ = 153.9 (C6), 151.1 (C2), 150.6 (C4), 127.5 (C8), 109.2 (C5), 43.3 (C11), 29.3 (C10), 15.7 (C12). – MS (MALDI, DHB): *m/z* = 274, 272 [1+H]⁺. – C₈H₉BrN₄O₂ (273.09 g mol⁻¹): calcd. C 35.18, H 3.32, N 20.52; found C 35.26, H 3.42, N 20.51.

4.3 General procedure for the synthesis of *trans*-[2] and *trans*-[3]

Equimolar amounts of compound **1** (66 mg, 0.24 mmol) and [M(PPh₃)₄] (0.24 mmol, M = Pd, Pt) were dissolved in toluene (10 mL) and stirred for three days under reflux. The solvent was then removed under reduced pressure and the residue washed twice each with hexane (10 mL each) and diethyl ether (10 mL each). After drying *in vacuo* the *trans*-configured complexes were obtained as colorless solids. Crystals suitable for X-ray diffraction studies were obtained by slow diffusion of diethyl ether into saturated dichloromethane solutions of the complexes.

4.3.1 Analytical data for *trans*-[2]: Yield: 144 mg (0.16 mmol, 67%). – ¹H NMR (400 MHz, CD₂Cl₂, ppm): δ = 8.44 (s, 1 H, H1), 7.62–7.57 (m, 12 H, Ph-*H*_{ortho}), 7.43 (t, ³J_{HH} = 7.3 Hz, 6 H, Ph-*H*_{para}), 7.34 (t, ³J_{HH} = 7.3 Hz, 12 H, Ph-*H*_{meta}), 3.83 (q, ³J_{HH} = 7.1 Hz, 2 H, H11), 3.09 (s, 3 H, H10), 0.97 (t, ³J_{HH} = 7.1 Hz, 3 H, H12). – ¹³C{¹H} NMR (101 MHz, CD₂Cl₂, ppm): δ = 163.7 (t, ²J_{CP} = 3.5 Hz, C8), 153.9 (C6), 152.8 (C2), 151.4 (C4), 135.0 (v-t, ²⁴J_{CP} = 6.6 Hz, Ph-*C*_{ortho}), 131.0 (Ph-*C*_{para}), 130.9 (v-t, ¹³J_{CP} = 24.3 Hz, Ph-*C*_{ipso}), 128.6 (v-t, ³⁵J_{CP} = 5.6 Hz, Ph-*C*_{meta}), 109.8 (C5), 43.9 (C11), 28.7 (C10), 15.9 (C12). – ³¹P{¹H} NMR (162 MHz, CD₂Cl₂, ppm): δ = 21.5 (s). – HRMS ((+)-ESI): *m/z* = 905.0845 (calcd. 905.0848 for C₄₄H₄₀BrN₄O₂P₂Pd, [trans-[2]+H]⁺), 927.06615 (calcd. 927.0668 for C₄₄H₃₉BrN₄O₂P₂PdNa, [trans-[2]+Na]⁺). – C₄₄H₃₉N₄BrO₂P₂Pd (904.03 g mol⁻¹): calcd. C 58.45, H 4.35, N 6.20; found C 56.72, H 4.40, N 5.96.

4.3.2 Analytical data for *trans*-[3]: Yield: 134 mg (0.13 mmol, 54%). – ¹H NMR (400 MHz, CD₂Cl₂, ppm): δ = 8.28 (s, 1 H, H1), 7.63–7.58 (m, 12 H, Ph-*H*_{ortho}), 7.45–7.42 (m, 6 H, Ph-*H*_{para}), 7.36–7.33 (m, 12 H, Ph-*H*_{meta}), 3.81 (q, ³J_{HH} = 7.1 Hz, 2 H, H11), 3.08 (s, 3 H, H10), 0.92 (t, ³J_{HH} = 7.1 Hz, 3 H, H12). – ¹³C{¹H} NMR (101 MHz, CD₂Cl₂, ppm): δ = 153.6 (C6), 152.9 (C2), 151.7 (t, ²J_{CP} = 9.8 Hz, C8), 151.2 (C4), 135.0 (v-t, ²⁴J_{CP} = 6.1 Hz, Ph-*C*_{ortho}), 131.1 (Ph-*C*_{para}), 130.1 (v-t, ¹³J_{CP} = 29.0 Hz, Ph-*C*_{ipso}), 128.5 (v-t, ³⁵J_{CP} = 5.3 Hz, Ph-*C*_{meta}), 108.3 (C5), 43.7 (C11), 28.7 (C10), 15.7 (C12). – ³¹P{¹H} NMR (162 MHz, CD₂Cl₂, ppm): δ = 18.7 (s, Pt satellites, ¹J_{PPt} = 2769 Hz). – HRMS ((+)-ESI): *m/z* = 993.1456 (calcd. 993.1451 for C₄₄H₄₀BrN₄O₂P₂Pt, [trans-[3]+H]⁺).

4.4 Complex *cis*-[3]

A solution of **1** (12.4 mg, 0.05 mmol) and [Pt(PPh₃)₄] (56.5 mg, 0.05 mmol) in toluene (10 mL) was stirred for one day at 110 °C. The solvent was then removed under reduced pressure and the residue was washed twice with hexane (5 mL each) and diethyl ether (5 mL each). After drying *in vacuo* compound *cis*-[3] was obtained as a colorless solid. Yield: 20 mg (0.02 mmol, 40%). – ¹H NMR (400 MHz, CD₂Cl₂-CD₃OD, ppm): δ = 7.48–7.39 (m, 12 H, Ph-*H*_{ortho}), 7.34–7.28 (m, 6 H, Ph-*H*_{para}), 7.21–7.12 (m, 12 H, Ph-*H*_{meta}), 4.66 (dq, ²J_{HH} = 14 Hz, ³J_{HH} = 7.1 Hz, 1 H, H11a), 4.13 (dq, ²J_{HH} = 14 Hz, ³J_{HH} = 7.1 Hz, 1 H, H11b), 3.24 (s, 3 H, H10), 1.56 (t, ³J_{HH} = 7.1 Hz, 3 H, H12). The proton H1 was not detected due to H/D-exchange with the solvent CD₃OD. – ¹³C{¹H} NMR (101 MHz, CD₂Cl₂-CD₃OD, ppm): δ = 167.6 (dd, ²J_{CP(trans)} = 148.9 Hz, ²J_{CP(cis)} = 9.5 Hz, C8), 154.0 (C6), 153.0 (d, ⁴J_{CP(trans)} = 10.2 Hz, C4), 151.7 (C2), 135.7 (d, ²J_{CP} = 10.4 Hz, P_{trans}Ph₃, Ph-*C*_{ortho}), 134.4 (d, ²J_{CP} = 11.2 Hz, P_{cis}Ph₃, Ph-*C*_{ortho}), 131.4 (d, ⁴J_{CP} = 2.2 Hz, P_{cis}Ph₃, Ph-*C*_{para}), 130.9 (d, ⁴J_{CP} = 2.2 Hz, P_{trans}Ph₃, Ph-*C*_{para}), 129.5 (dd, ¹J_{CP} = 63.0 Hz, ²J_{CP} = 1.5 Hz, P_{trans}Ph₃, Ph-*C*_{ipso}), 128.6 (d, ³J_{CP} = 11.3 Hz, P_{cis}Ph₃, Ph-*C*_{meta}), 128.5 (d, ³J_{CP} = 10.4 Hz, P_{trans}Ph₃, Ph-*C*_{meta}), 108.7 (d, ⁴J_{CP(trans)} = 4.0 Hz, C5), 44.3 (C11), 30.1 (C10), 15.7 (C12). The signal for C_{ipso} of P_{cis}Ph₃ was not detected. – ³¹P{¹H} NMR (162 MHz, CD₂Cl₂-CD₃OD, ppm): δ = 15.3 (d, ²J_{PP} = 17.9 Hz, Pt satellites ¹J_{PPt} = 1973 Hz, P_{trans}Ph₃), 12.6 (d, ²J_{PP} = 18.0 Hz, Pt satellites ¹J_{PPt} = 3970 Hz, P_{cis}Ph₃).

4.5 General procedure for the synthesis of complexes *trans*-[4]BF₄ and *trans*-[5]BF₄

Samples of complexes *trans*-[2] or *trans*-[3] (0.07 mmol) were suspended in THF (5 mL) and an excess of HBF₄·Et₂O (0.030 mL, 0.22 mmol) was added dropwise to the stirred suspension. The reaction mixture was stirred for 1 h at ambient temperature, while the suspension became a clear solution. The solvent was then removed under reduced pressure and the residue was washed twice with diethyl ether (10 mL each). After drying of the residue *in vacuo* the pNHC complexes were obtained as colorless solids. Crystals of *trans*-[4]BF₄ and *trans*-[5]BF₄ suitable for X-ray diffraction experiments were obtained by slow diffusion of Et₂O into a saturated acetonitrile-methanol or acetonitrile solution of the individual complexes.

4.5.1 Analytical data for *trans*-[4]BF₄: Yield: 57% (40 mg, 0.04 mmol). – ¹H NMR (400 MHz, CD₃CN-CD₃OD, ppm): δ = 11.25 (s, 1 H, H9), 9.90 (s, 1 H, H1), 7.66 (m, 12 H, Ph-*H*_{ortho}), 7.54 (t, ³J_{HH} = 7.3 Hz, 6 H, Ph-*H*_{para}), 7.47 (t, ³J_{HH} = 7.3 Hz, 12 H, Ph-*H*_{meta}), 3.99 (q, ³J_{HH} = 7.2 Hz, 2 H, H11), 2.92 (s, 3 H, H10), 0.96 (t, ³J_{HH} = 7.2 Hz, 3 H, H12). – ¹³C{¹H} NMR (101 MHz, CD₃CN-CD₃OD, ppm): δ = 164.9 (t, ²J_{CP} = 9.4 Hz, C8), 152.9 (C6), 149.8 (C2), 144.8 (C4), 135.6 (v-t, ²⁴J_{CP} = 6.3 Hz, Ph-*C*_{ortho}), 130.5 (Ph-*C*_{para}), 130.2 (v-t, ¹³J_{CP} = 25.7 Hz, Ph-*C*_{ipso}), 130.1 (v-t, ³⁵J_{CP} = 5.4 Hz, Ph-*C*_{meta}), 109.5 (C5), 48.1 (C11), 30.7 (C10), 15.7 (C12). – ³¹P{¹H} NMR (162 MHz, CD₃CN-CD₃OD, ppm): δ = 21.0 (s). – HRMS ((+)-ESI): *m/z* = 905.0842 (calcd. 905.0848 for C₄₄H₄₀N₄BrO₂P₂Pd, [trans-[4]⁺]).

4.5.2 Analytical data for *trans*-[5]BF₄: Yield: 43% (28 mg, 0.03 mmol). – ¹H NMR (400 MHz, CD₃CN, ppm): δ = 10.41 (s, 1 H, H9), 8.98 (s, 1 H, H1), 7.70–7.68 (d, ³J_{HH} = 7.3 Hz, 12 H, Ph-*H*_{ortho}), 7.57–7.54 (m, 6 H, Ph-*H*_{para}), 7.51–7.48 (m, 12 H, Ph-*H*_{meta}), 3.99 (q, ³J_{HH} = 7.0 Hz, 2 H, H11), 2.91 (s, 3 H, H10), 0.97 (t, ³J_{HH} = 7.1 Hz, 3 H, H12). – ¹³C{¹H} NMR (101 MHz, CD₃CN, ppm): δ = 152.7 (C6), 151.7 (t, ²J_{CP} = 10.1 Hz, C8), 149.5

(C2), 143.8 (C4), 135.5 (ν -t, $^2J_{CP} = 6.1$ Hz, Ph-C_{ortho}), 132.9 (Ph-C_{para}), 129.9 (ν -t, $^3J_{CP} = 5.4$ Hz, Ph-C_{meta}), 129.3 (ν -t, $^1J_{CP} = 29.8$ Hz, Ph-C_{ipso}), 108.3 (C5), 47.6 (C11), 30.7 (C10), 15.3 (C12). – $^{31}\text{P}\{^1\text{H}\}$ NMR (162 MHz, CD₃CN, ppm): $\delta = 16.6$ (s, Pt satellites $^1J_{PPt} = 2464$ Hz). – ^{195}Pt NMR (86 MHz, CD₃CN, ppm): $\delta = -4500.4$ (t, $^1J_{PPt} = 2464$ Hz). – HRMS ((+)-ESI): $m/z = 993.1445$ (calcd. 993.1451 for C₄₄H₄₀N₄BrO₂P₂Pt, [trans-5])⁺.

4.6 Complex mixture *cis*-/*trans*-[5]BF₄

A mixture of *cis*-[3]/*trans*-[3] in the ratio of 1:0.54 (95 mg, 0.10 mmol) was suspended in THF (5 mL) and an excess of HBF₄·Et₂O (0.030 mL, 0.22 mmol) was added under stirring to the suspension. The reaction mixture became a clear solution while stirring at ambient temperature for 1 h. After removal of the solvent under reduced pressure, the obtained solid was washed twice with diethyl ether (10 mL each) and dried *in vacuo*. The obtained colorless mixture of *cis*-/*trans*-[5]BF₄ exhibited the same ratio of *cis*- and *trans*-isomer as observed for the starting material. Yield: 50 mg (0.05 mmol, 50%). Analytical data assigned to *trans*-[5] in the mixture are identical to those of a pure sample of *trans*-[5]BF₄ (see above). Therefore, only data for *cis*-[5]BF₄ are listed here. – ^1H NMR (400 MHz, CD₃CN, ppm): $\delta = 11.01$ (s, 1 H, H9), 9.02 (s, 1 H, H1), 7.55–7.49 (m, 12 H, Ph-H_{ortho} of P_{cis}Ph₃ and P_{trans}Ph₃), 7.55–7.42 (m, 18 H, Ph-H_{para/meta}), 4.58 (dq, $^2J_{HH} = 14$ Hz, $^3J_{HH} = 7.1$ Hz, 1 H, H11a), 4.21 (dq, $^2J_{HH} = 14$ Hz, $^3J_{HH} = 7.1$ Hz, 1 H, H11b), 3.26 (s, 3 H, H10), 1.55 (t, $^3J_{HH} = 7.1$ Hz, 3 H, H12). – $^{13}\text{C}\{^1\text{H}\}$ NMR (101 MHz, CD₃CN, ppm): $\delta = 164.6$ (dd, $^2J_{CP(\text{trans})} = 145.4$ Hz, $^2J_{CP(\text{cis})} = 9.6$ Hz, C8), 153.2 (C6), 150.0 (C2), 144.2 (d, $^4J_{CP(\text{trans})} = 5.8$ Hz, C4), 136.3 (d, $^2J_{CP} = 10.2$ Hz, Ph-C_{ortho}, P_{trans}Ph₃), 134.9 (d, $^2J_{CP} = 11.2$ Hz, Ph-C_{ortho}, P_{cis}Ph₃), 133.1 (d, $^4J_{CP} = 2.1$ Hz, Ph-C_{para}, P_{cis}Ph₃), 132.2 (d, $^4J_{CP} = 2.0$ Hz, Ph-C_{para}, P_{trans}Ph₃), 130.0–129.9 (m, Ph-C_{meta}, P_{cis}Ph₃), 29.3 (d, $^3J_{CP} = 10.7$ Hz, Ph-C_{meta}, P_{trans}Ph₃), 108.5 (d, $^4J_{CP(\text{trans})} = 4.0$ Hz, C5), 47.4 (C11), 30.9 (C10), 15.2 (C12). The signals for C_{ipso} of the PPh₃ ligands were not detected. – $^{31}\text{P}\{^1\text{H}\}$ NMR (162 MHz, CD₃CN, ppm): $\delta = 13.1$ (d, $^2J_{PP} = 18.9$ Hz, Pt satellites $^1J_{PPt} = 2286$ Hz, P_{trans}Ph₃), 11.0 (d, $^2J_{PP} = 18.9$ Hz, Pt satellites $^1J_{PPt} = 3652$ Hz, P_{cis}Ph₃). – ^{195}Pt NMR (86 MHz, CD₃CN, ppm): $\delta = -4602.9$ (dd, $^1J_{P(\text{cis})Pt} = 3652$ Hz, $^1J_{P(\text{trans})Pt} = 2286$ Hz). – MS ((+)-ESI): $m/z = 993.1445$ (calcd. 993.1451 for [cis-/*trans*-5])⁺.

4.7 X-ray structure determinations

Diffraction data for all compounds were collected with a Bruker APEX-II CCD diffractometer equipped with a micro source using MoK α radiation ($\lambda = 0.71073$ Å). Diffraction data was collected at $T = 100(2)$ K over the full sphere and was corrected for absorption. Structure solutions were found with the SHELXT (intrinsic phasing) [40] package (intrinsic phasing) using direct methods and were refined with SHELXL [41] against all $|F^2|$ using first isotropic and later anisotropic displacement parameters (for exceptions see description of the individual molecular structures). Hydrogen atoms were added to the structure models on calculated positions if not noted otherwise.

4.7.1 Selected crystallographic details for *trans*-[2]·2CH₂Cl₂:

Formula C₄₆H₄₃N₄BrCl₄O₂P₂Pd, $M = 1073.89$ g·mol⁻¹, colorless block, $0.50 \times 0.44 \times 0.44$ mm³, triclinic, space group $P\bar{1}$, $Z = 2$, $a = 12.0828(3)$, $b = 14.6597(4)$, $c = 15.0360(4)$ Å, $\alpha = 98.3120(10)$, $\beta = 90.9220(10)$, $\gamma = 112.3940(10)^\circ$, $V = 2429.23(11)$ Å³, $\rho_{\text{calcd}} = 1.47$ g·cm⁻³, $\mu = 1.5$ mm⁻¹, ω

and φ scans, 71,425 measured intensities ($6.5^\circ \leq 2\theta \leq 60.9^\circ$), semi-empirical absorption correction ($0.561 \leq T \leq 0.746$), 14,697 independent intensities ($R_{\text{int}} = 0.0351$) and 12,839 observed intensities ($I \geq 2\sigma(I)$), refinement of 533 parameters against $|F^2|$ of all independent intensities with hydrogen atoms on calculated positions. $R = 0.0395$, $R_w = 0.1086$, $R_{\text{all}} = 0.0467$, $R_{w,\text{all}} = 0.1132$. The asymmetric unit contains one formula unit of *trans*-[2] and two molecules of CH₂Cl₂. One of the CH₂Cl₂ molecules is disordered and no hydrogen positions were calculated for this molecule.

4.7.2 Selected crystallographic details for *trans*-[3]·2CH₂Cl₂:

Formula C₄₆H₄₃N₄BrCl₄O₂P₂Pt, $M = 1162.58$ g·mol⁻¹, colorless block, $0.35 \times 0.30 \times 0.27$ mm³, triclinic, space group $P\bar{1}$, $Z = 2$, $a = 12.0703(4)$, $b = 14.6120(5)$, $c = 15.0404(5)$ Å, $\alpha = 98.122(2)$, $\beta = 91.113(2)$, $\gamma = 112.257(2)^\circ$, $V = 2422.71(14)$ Å³, $\rho_{\text{calcd}} = 1.59$ g·cm⁻³, $\mu = 4.0$ mm⁻¹, ω and φ scans, 68,108 measured intensities ($7.1^\circ \leq 2\theta \leq 66.3^\circ$), semi-empirical absorption correction ($0.332 \leq T \leq 0.408$), 18,290 independent intensities ($R_{\text{int}} = 0.0537$) and 15,011 observed intensities ($I \geq 2\sigma(I)$), refinement of 533 parameters against $|F^2|$ of all independent intensities with hydrogen atoms on calculated positions. $R = 0.0438$, $R_w = 0.1027$, $R_{\text{all}} = 0.0603$, $R_{w,\text{all}} = 0.1094$. The asymmetric unit contains one formula unit of *trans*-[3] and two molecules of CH₂Cl₂. One of the CH₂Cl₂ molecules is disordered and no hydrogen positions were calculated for this molecule.

4.7.3 Selected crystallographic details for *trans*-[4]BF₄:

Formula C₄₄H₄₀N₄BBBrF₄O₂P₂Pd, $M = 991.86$ g·mol⁻¹, colorless block, $0.20 \times 0.06 \times 0.06$ mm³, triclinic, space group $P\bar{1}$, $Z = 4$, $a = 10.8912(3)$, $b = 13.4347(4)$, $c = 31.4189(8)$ Å, $\alpha = 77.962(2)$, $\beta = 89.938(2)$, $\gamma = 66.2390(10)^\circ$, $V = 4097.3(2)$ Å³, $\rho_{\text{calcd}} = 1.61$ g·cm⁻³, $\mu = 1.6$ mm⁻¹, ω and φ scans, 119,653 measured intensities ($3.9^\circ \leq 2\theta \leq 61.0$), semi-empirical absorption correction ($0.744 \leq T \leq 0.912$), 24,881 independent intensities ($R_{\text{int}} = 0.0666$) and 20,818 observed intensities ($I \geq 2\sigma(I)$), refinement of 1079 parameters against $|F^2|$ of all independent intensities with hydrogen atoms on calculated positions. $R = 0.0433$, $R_w = 0.0951$, $R_{\text{all}} = 0.0589$, $R_{w,\text{all}} = 0.1029$. The asymmetric unit contains two formula unit of *trans*-[4]BF₄.

4.7.4 Selected crystallographic details for *trans*-[5]BF₄·C₄H₁₀O:

Formula C₄₈H₅₀N₄BBBrF₄O₃P₂Pt, $M = 1154.67$ g·mol⁻¹, colorless needle, $0.46 \times 0.17 \times 0.04$ mm³, triclinic, space group $P\bar{1}$, $Z = 2$, $a = 10.1468(3)$, $b = 14.1862(3)$, $c = 16.7879(4)$ Å, $\alpha = 89.7850(10)$, $\beta = 82.6430(10)$, $\gamma = 89.0930(10)^\circ$, $V = 2396.33(10)$ Å³, $\rho_{\text{calcd}} = 1.60$ g·cm⁻³, $\mu = 3.89$ mm⁻¹, ω and φ scans, 79,641 measured intensities ($5.0^\circ \leq 2\theta \leq 61.1$), semi-empirical absorption correction ($0.545 \leq T \leq 0.746$), 14,572 independent intensities ($R_{\text{int}} = 0.0509$) and 12,676 observed intensities ($I \geq 2\sigma(I)$), refinement of 572 parameters against $|F^2|$ of all independent intensities with hydrogen atoms on calculated positions. $R = 0.0351$, $R_w = 0.0921$, $R_{\text{all}} = 0.0443$, $R_{w,\text{all}} = 0.0965$. The asymmetric unit contains one formula unit of *trans*-[5]BF₄ and one Et₂O molecule.

Further details of the crystal structure investigation may be obtained from Fachinformationszentrum Karlsruhe, 76344 Eggenstein-Leopoldshafen, Germany (fax: +49-7247-808-666; E-mail: crysdata@fiz-karlsruhe.de, http://www.fiz-informationsdienste.de/en/DB/icsd/depot_anforderung.html) on quoting the deposition number CCDC 2058003 (*trans*-[2]·2CH₂Cl₂), CCDC 2058004 (*trans*-[3]·2CH₂Cl₂), CCDC 20058006 (*trans*-[4]BF₄) and CCDC 2058005 (*trans*-[5]BF₄·C₄H₁₀O).

Author contributions: All the authors have accepted responsibility for the entire content of this submitted manuscript and approved submission.

Research funding: This research was funded by Deutsche Forschungsgemeinschaft (SFB 858 and IRTG 2027).

Conflict of interest statement: The authors declare no conflicts of interest regarding this article.

References

1. Hahn F. E., Jahnke M. C. *Angew. Chem. Int. Ed.* 2008, *47*, 3122–3172.
2. Jahnke M. C., Hahn F. E. *Top. Organomet. Chem.* 2010, *30*, 95–129.
3. Hopkinson M. N., Richter C., Schedler M., Glorius F. *Nature* 2014, *510*, 485–496.
4. Janssen-Müller D., Schlepphorst C., Glorius F. *Chem. Soc. Rev.* 2017, *46*, 4845–4854.
5. Mata J. A., Hahn F. E., Peris E. *Chem. Sci.* 2014, *5*, 1723–1732.
6. Peris E. *Chem. Rev.* 2018, *118*, 9988–10031.
7. Liu W., Gust R. *Coord. Chem. Rev.* 2016, *329*, 191–213.
8. Sinha N., Hahn F. E. *Acc. Chem. Res.* 2017, *50*, 2167–2184.
9. Gan M.-M., Liu J.-Q., Zhang L., Wang Y.-Y., Hahn F. E., Han Y.-F. *Chem. Rev.* 2018, *118*, 9587–9641.
10. Jahnke M. C., Hahn F. E. *Coord. Chem. Rev.* 2015, *293-294*, 95–115.
11. Jahnke M. C., Hahn F. E. *Chem. Lett.* 2015, *44*, 226–237.
12. Kuwata S., Hahn F. E. *Chem. Rev.* 2018, *118*, 9642–9677.
13. Edwards P. G., Hahn F. E. *Dalton Trans.* 2011, *40*, 10278–10288.
14. Das R., Hepp A., Daniliuc C. G., Hahn F. E. *Organometallics* 2014, *33*, 6975–6987.
15. Meier N., Hahn F. E., Pape T., Siering C., Waldvogel S. R. *Eur. J. Inorg. Chem.* 2007, 1210–1214; <https://doi.org/10.1002/ejic.200601258>.
16. Miranda-Soto V., Grotjahn D. B., DiPasquale A. G., Rheingold A. L. *J. Am. Chem. Soc.* 2008, *130*, 13200–13201.
17. Marelus D. C., Darrow E. H., Moore C. E., Golen J. A., Rheingold A. L., Grotjahn D. B. *Chem. Eur J.* 2015, *21*, 10988–10992.
18. Hahn F. E. *ChemCatChem* 2013, *5*, 419–430.
19. Tan K. L., Bergman R. G., Ellman J. A. *J. Am. Chem. Soc.* 2002, *124*, 3202–3203.
20. He F., Wesolek M., Danopoulos A. A., Braunstein P. *Chem. Eur J.* 2016, *22*, 2658–2671.
21. Price C., Elsegood M. R. J., Clegg W., Rees N. H., Houlton A. *Angew. Chem. Int. Ed. Engl.* 1997, *36*, 1762–1764.
22. Flowers S. E., Johnson M. C., Pitre B. Z., Cossairt B. M. *Dalton Trans.* 2018, *47*, 1276–1283.
23. Brackemeyer D., Schulte to Brinke C., Roelfes F., Hahn F. E. *Dalton Trans.* 2017, *46*, 4510–4513.
24. Mühlen C., Linde J., Rakers R., Tan T. T. Y., Kampert F., Glorius F., Hahn F. E. *Organometallics* 2019, *38*, 2417–2421.
25. Cepa S., Schulte to Brinke C., Roelfes F., Hahn F. E. *Organometallics* 2015, *34*, 5454–5460.
26. Fraser P. J., Roper W. R., Stone F. G. A. *J. Chem. Soc., Dalton Trans.* 1974, 102–105.
27. Fraser P. J., Roper W. R., Stone F. G. A. *J. Organomet. Chem.* 1973, *50*, C54–C56.
28. Kösterke T., Pape T., Hahn F. E. *J. Am. Chem. Soc.* 2011, *133*, 2112–2115.
29. Blumenberg J., Wilm L. F. B., Hahn F. E. *Organometallics* 2020, *39*, 1281–1287.
30. Branzan R. M. C., Kösters J., Jahnke M. C., Hahn F. E. *Z. Naturforsch* 2016, *71b*, 1077–1085.
31. Jin H., Tan T. T. Y., Hahn F. E. *Angew. Chem. Int. Ed.* 2015, *54*, 13811–13815.
32. Jin H., Mück-Lichtenfeld C., Hepp A., Stephan D. W., Hahn F. E. *Chem. Eur J.* 2017, *23*, 5943–5947.
33. Termühlen S., Blumenberg J., Hepp A., Daniliuc C. G., Hahn F. E. *Angew. Chem. Int. Ed.* 2021, *60*, 2599–2602.
34. Jahnke M. C., Hervé A., Kampert F., Hahn F. E. *Inorg. Chim. Acta* 2021, *515*, 120055.
35. Brackemeyer D., Hervé A., Schulte to Brinke C., Jahnke M. C., Hahn F. E. *J. Am. Chem. Soc.* 2014, *136*, 7841–7844.
36. Kampert F., Brackemeyer D., Tan T. T. Y., Hahn F. E. *Organometallics* 2018, *37*, 4181–4185.
37. Klein J. P., Klaus J. S., Kumar A. M., Gong B. *U. S. Jpn. Outlook* 2005, *6*, 878–715 B1.
38. Dutschke P. D., Bente S., Daniliuc C. G., Kinas J., Hepp A., Hahn F. E. *Dalton Trans.* 2020, *49*, 14388–14392.
39. Kösterke T., Kösters J., Würthwein E.-U., Mück-Lichtenfeld C., Schulte to Brinke C., Lahoz F., Hahn F. E. *Chem. Eur J.* 2012, *18*, 14594–14598.
40. Sheldrick G. M. *Acta Crystallogr.* 2015, *A71*, 3–8.
41. Sheldrick G. M. *Acta Crystallogr.* 2015, *C71*, 3–8.